ISTITUTO NAZIONALE DI FISICA NUCLEARE
Laboratori Nazionali di Frascati

LNF-79/67(R)
22 Ottobre 1979

G. P. Capitani, E. De Sanctis, P. Di Giacomo, S. Gentile, C. Guaraldo, V. Lucherini, E. Polli, A. R. Reolon and R. Scrimaglio: RANGE TELESCOPE FOR PROTONS TO INVESTIGATE (γ, p) REACTIONS USING THE MONOCHROMATIC PHOTON BEAM OF FRASCATI LEALE LABORATORY.

Servizio Documentazione
dei Laboratori Nazionali di Frascati
Cas. Postale 13 - Frascati (Roma)

INFN - Laboratori Nazionali di Frascati
Servizio Documentazione

LNF-79/67(R)
22 Ottobre 1979

G. P. Capitani, E. De Sanctis, P. Di Giacomo, S. Gentile, C. Guaraldo, V. Lucherini, E. Polli, A. R. Reolon and R. Scrimaglio: RANGE TELESCOPE FOR PROTONS TO INVESTIGATE (γ, p) REACTIONS USING THE MONOCHROMATIC PHOTON BEAM OF FRASCATI LEALE LABORATORY.

1. - INTRODUCTION.

One of the aims of the research program performed using the monochromatic photon beam of the LNF LEALE Laboratory - a collaboration with the Sezione INFN of Genova - is the study of (γ, p) reactions on light nuclei: d, ^{3}He, ^{4}He[1].

The interest of such investigation arises from the fact that for photon energies above 50 MeV the experimental data of any of the above reactions do not agree among themselves. Moreover, for energies above 60 MeV the data do not agree with theories which do not take into account interaction effects in nuclei[2]. Indeed, the experimental cross section integrated up to meson photoproduction threshold has an higher value than that obtained by classic sum rules. Modern theories consider explicitly isobaric configurations in nuclei, either by supposing the possibility of the existence of excited nucleons N^* inside the nucleus - isobaric configuration (IC) of the nucleus - or by adding mesonic exchange currents (MEC) to the electromagnetic photon-nucleus interaction potential. By means of energetic photons ($E_\gamma \geq 140$ MeV) we are able to explore regions of one fermi dimensions, in which such interaction effects probably occur: in other words, photon-nucleus interaction is sensitive to the high momentum components of the nuclear wave function and allows to obtain some informations also about N-N^* and N^*-N^* short-range correlations. From here, the importance of the study of light nuclei arises, especially of the deuteron, which can be considered as fundamental point "to go to Relativistic Nuclear Physics (RNP) or, in other words, in order to do the Quantum Field Theory (QFT) of the nucleus"[3].

Deuteron photodisintegration experiment is at present data taking in LEALE Laboratory[4].

The experimental apparatus used to detect photoprotons is reported in Fig. 1. It is made up of:

- Four E, dE/dx telescopes, at different angles, to detect protons of energies ≤ 120 MeV. Each telescope consists of two scintillators: the first one is a plastic scintillator ($10 \times 10 \times 0.3$ cm^3) and it is used to measure the energy loss for unitary path; the second one is a NaI (Tl) scintillator (cylinder shaped, 6 cm high, 12 cm basic diameter) and measures the total energy loss of the protons.
- One range hodoscope-telescope (eight angular channels and seven energy channels) to detect protons of energy ≥ 80 MeV.

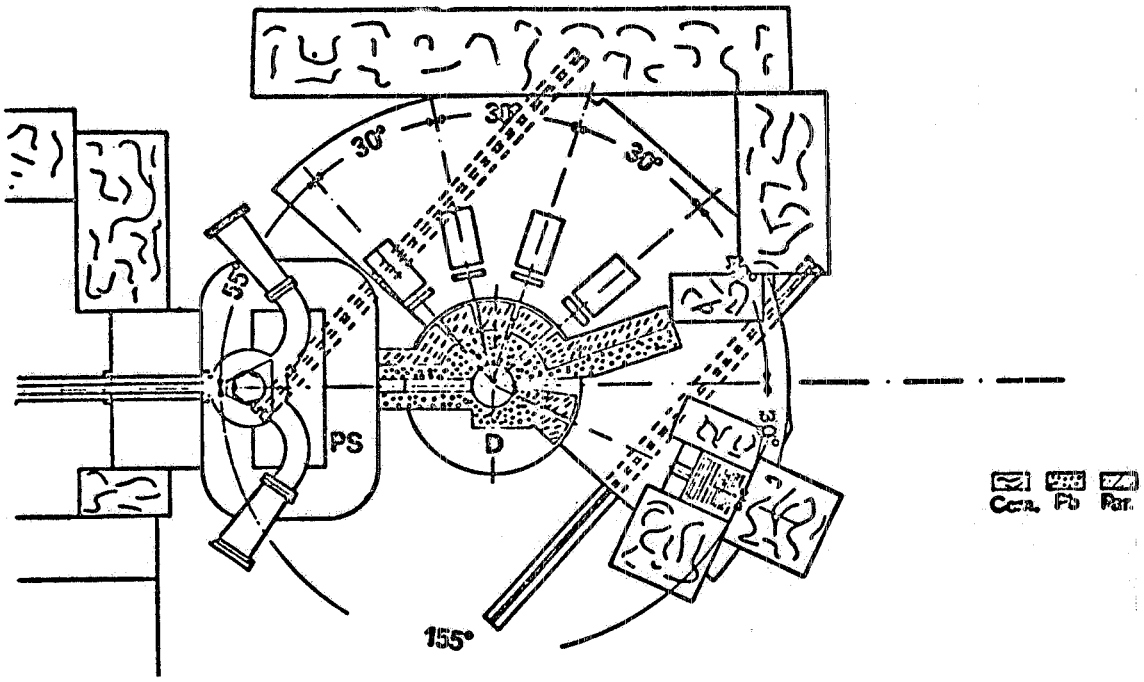

FIG. 1 - The experimental set up for D(γ, p)n reaction. PS: pair spectrometer; D:deuteron target. Four E, dE/dx telescope and a range telescope are placed at different angles on a movable platform.

The description of features and performances of E, dE/dx telescopes has been already reported elsewhere[5].

In this paper we describe in some detail geometric characteristics and logical performances of the range telescope and of the hodoscope (Sect. 2), the electronic coupling and the data collecting system (Sect. 3). In Section 4 the calculations of the telescope response obtained by a Monte Carlo method and proton energy spectra from deuteron photodisintegration are reported.

2. - THE RANGE TELESCOPE AND THE HODOSCOPE.

2.1. - Range telescope.

The range telescope is made up of 11 scintillator counters (type NE 102 A ; photomultipliers Philips 56AVP) and a plexiglas Čerenkov counter (refractive index : 1.49 ; two Philips 56AVP photomultipliers). Counters arrangement is sketched in Fig. 2.

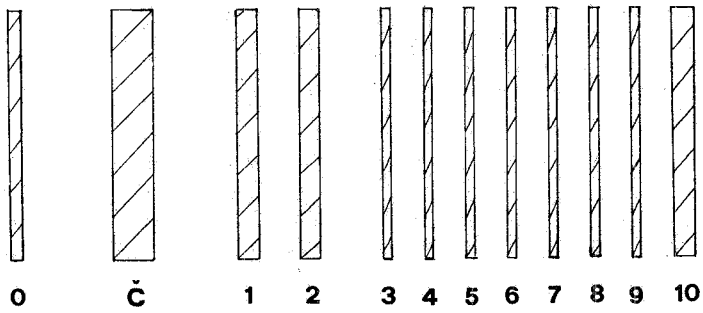

Scintillators	Thickness (mm)	Size (cm^2)
0,3,4,5,6,7,8,9	2	30x30
1,2,10	5	"
Čerenkov	50	"

FIG. 2 - Sketched configuration of range telescope and scintillator dimensions.

Through the use of light pipes properly shaped and shifted, the overall system results quite compact (lenght along proton flux direction: 30 cm).

TABLE I - Energy values calculated for protons incoming in each channel.

Counter	Channel	Energy values	
		(a)	(b)
3	1	95.42	100.73
4	2	97.35	102.59
5	3	99.25	104.42
6	4	101.12	106.22
7	5	102.97	108.01
8	6	104.80	109.78
9	7	106.60	111.52

(a) without hodoscope counters;
(b) with hodoscope counters;
(a) and (b) configurations are in absence of any absorber.

The function of the different counters is the following:

- the 0 counter is used to reduce the neutral particle background;
- the $\check{C}$ counter eliminates electrons and pions of kinetic energy $\geq$49 MeV with an efficiency of 98%;
- the 1 and 2 counters are used to discriminate among particles by their pulse-height spectra;
- the 3÷9 counters define energy channels of width ranging from 1.3 to 2 MeV;
- the 10 counter selects the passing protons, i.e. defines the maximum range of events in the telescope.

In Table I (column (a)) the energy values for protons incoming into each channel are reported: in this case the counters are placed as in Fig. 2.

Obviously it is possible to raise either the threshold of the telescope or the width of each channel, by inserting suitable absorbers before the 0 counter and between the counters that define the energy channels. In fact, in order to not reduce the efficiency of the 0 counter, the first absorber is placed between the 0 and the Cerenkov counter.

2.2. - Hodoscope.

To determine the angle of collected protons a hodoscope is inserted before the 0 counter of the telescope. The hodoscope is made up of 8 scintillator counters (type NE102; photomultipliers Philips 56AVP) placed on two planes, as shown in Fig. 3a; each counter has two scintillator strips, mutually arranged as shown in Fig. 3b.

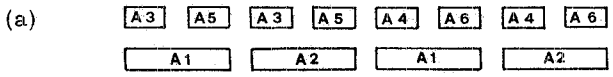

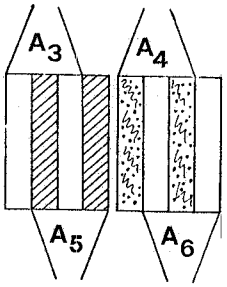

COUNTERS	SCINTILLATOR DIMENSIONS
$A_1 \cdot A_2$	$60 \times 3 \times 160\ mm^3$
$A_3 \div A_6$	$30 \times 3 \times 160\ mm^3$

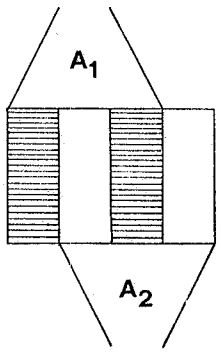

FIG. 3 - Hodoscope configuration: scintillators planes and dimensions (a); scintillator strips arrangement (b).

The hodoscope defines 8 angular channels, by suitable coincidence between the counters of the two planes (see Table II). Each angular channel is 4° large, for a distance target - first plane of 10.4 cm.

TABLE II - Hodoscope angular channels.

Coincidence	Angle (degree)	Coincidence	Angle (degree)
$A_1 A_3$	24.15	$A_1 A_4$	30.84
$A_1 A_5$	25.82	$A_1 A_6$	32.5
$A_2 A_3$	27.5	$A_2 A_4$	34.18
$A_2 A_5$	29.17	$A_2 A_6$	35.85

The energy uncertainty due to the finite angular widths and to the vertical dimensions of the scintillators is lower than 1.5 %; the same amount of uncertainty is due to the finite dimensions of deuteron target (cylinder diameter: 4 cm).

In column (b) of Table I the energy values for protons incoming into each telescope channel in the configuration with the hodoscope inserted are reported.

3. - ELECTRONICS AND ON-LINE ANALYSIS.

IN Fig. 4 the electronic coupling is reported. The data acquisition is performed on-line on the PDP-15 computer of LEALE Laboratory.

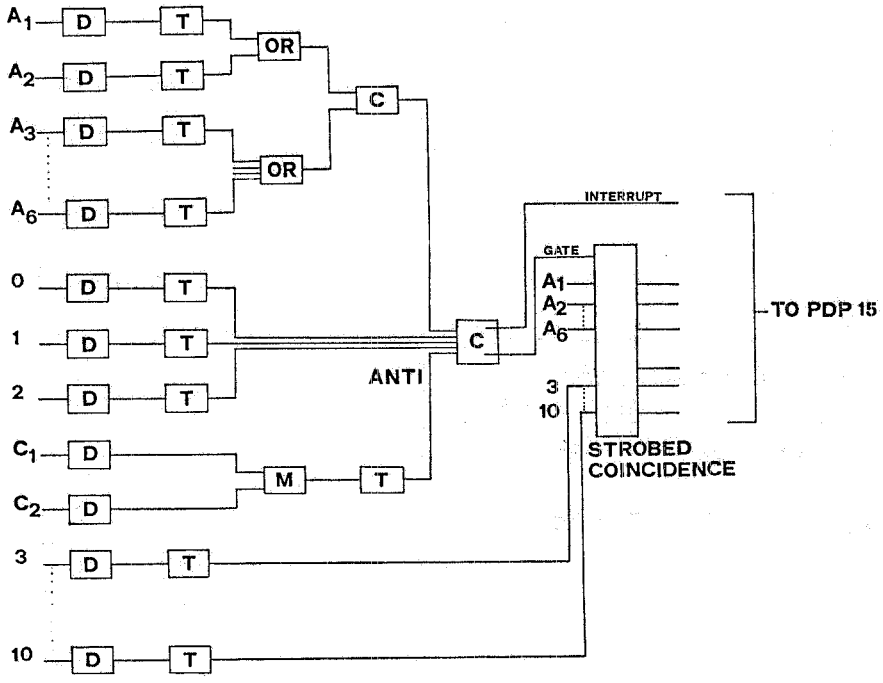

FIG. 4 - Electronic logical coupling. D: delay; T: discriminator trigger; C: coincidence; M: mixer.

The trigger configuration is $(0, 1, 2, \check{C}, A)$, where A is the coincidence between one of the angular counters of the first plane and one of the angular counters of the second plane of the hodoscope. The trigger opens a gate which enables the transmission to computer of the signals from the range telescope and the hodoscope (strobed coincidence). Each event resulting from any configuration which is different from those of Table II is considered a "bad one" and is no longer elaborated.

To assigne the proton range one should calculate[6] the probability that each of 8 ideal configurations has to form the measured pattern and assume as "true pattern" that which has the highest probability. This criterion has the advantage to associate to the real pattern the most reliable among the ideal ones and the corresponding reliabilities; the disadvantage is that it takes too long time for an on-line analysis. Therefore, a different criterion has been used for on-line analysis. We assume the proton is stopped in the first counter which gives a signal and is followed by at least two counters without a signal. It results that such a criterion differs from that of ref. (6) by no more than 1 % in the worst case.

4. - RESPONSE FUNCTION OF THE RANGE TELESCOPE.

The response function of the range telescope has been evaluated by a Monte Carlo calculation which took into account the energy loss of protons and the spectrum distorsion due to nuclear interactions, multiple scattering and straggling.

4.1. - Nuclear interactions.

The probability that proton interact with nuclei of telescope material has been calculated by the expression:

$$\alpha = 100 \left[1 - \frac{100 - \alpha(E_i)}{100 - \alpha(E_f)} \right]$$

where:

- $\alpha(E_i)$ is the percentage of protons, of energy E_i, having nuclear interactions in the range $R(E_i)$;
- $\alpha(E_f)$ is the percentage of protons which have nuclear interactions in the range $R(E_f)$, where E_f is the energy of the outgoing protons;
- α is the percentage of protons which have nuclear interactions, with incoming energy E_i and outgoing energy E_f.

The values of $\alpha(E_i)$ and $\alpha(E_f)$ have been obtained from a best fit of the percentage nuclear absorption values reported in the Tables of ref. (7). For proton energies below 100 MeV the fit is obtained by a fourth order polinomial; for energies above 100 MeV by a straight line.

4.2. - Multiple scattering.

Multiple scattering contributions have been evaluated following the Nigam and Sundaresam theory, in the approximate formulation given by Marion and Zimmerman[8]. This approximation is accurate for medium energy particles scattered by materials of moderate thickness.

According to this theory, the distribution of the root mean square angle θ of multiple scattering is approximately a Gaussian one and is given by:

$$F(x) \propto \exp(-x^2/x_w^2) \tag{1}$$

where

$$x = \theta / \chi_c B^{1/2}, \tag{2}$$

$$\chi_c = 0.1569 \frac{Z(Z+1)z^2 t}{A(pv)^2} \tag{3}$$

B is a root of $B - \ln B = b$

(The theory is valid for $4 \lesssim B \lesssim 15$);

$$b = \ln\left[2730\,(Z+1)\,Z^{1/3}\,z^2\,t/A\beta^2\right] - 0.1544\,;$$

$$\beta^2 = 1 - (1 + E/Mc^2)\,;$$

E and Mc^2 are kinetic energy and rest mass of incident particle;

Z = atomic number of scatterer;

z = atomic number of incident particle;

A = atomic weight of scatterer;

t = thickness of scattering foil (gr/cm^2);

pv = momentum-velocity product of incident particle in MeV.

The parameter x_w gives the angle $\theta_{1/e}$ at which the angular distribution is reduced to 1/e of its value at $x = 0$. It is a function of B. B values as a function of b are reported in Tables in ref. (8). In the same reference the behaviour of x_w versus B is reported. B(b) and $x_w(B)$ have been evaluated using, respectively, a fourth order and a third order polinomial, of which the coefficients have been calculated from best fits of the quoted values.

From the relation

$$\theta_{1/e} = \chi_c B^{1/2}\, x_w(B) \qquad (2')$$

the $\theta_{1/e}$ angle is deduced. Then the variance $\sigma = \theta_{1/e}/\sqrt{2}$ of Gaussian distribution of multiple angle scattering is obtained.

The subsequent steps of the routine are the assumption that the proton is scattered at an angle θ in the middle of the path and the random extraction of the distribution of the φ angle. The outgoing protons coordinates for a given material and the proton energy loss, taking into account different path of the scattered particle, are finally calculated.

4.3. - Straggling.

Uncertainties in the proton range due to straggling in telescope materials have been taken into account by assuming a Gaussian shaped range distribution, of which the variance σ_o is given by[8]:

$$\sigma_o = R_o\,(102.2/Mc^2)^{1/2}\, f(E/Mc^2)\,,$$

where R_o is the mean range of the proton and f is a function which is different for various materials. We have used the graphs of $f(E/Mc^2)$ valid for particles stopping in iron and σ_o/R_o values for aluminum, copper and beryllium, relatively to iron, reported in ref. (8). The values of σ_o/R_o for CH have been obtained from those for Be and Al by linear interpolation.

The uncertainty ΔR on the range R_o of a proton of energy E is extracted by the routine from a Gaussian distribution of variance σ_o and mean value 0.

Straggling correction is not applied if the proton is absorbed for nuclear interaction or if it leaves the telescope because of multiple scattering or because of large incidence angle.

In Table III the range telescope response for different energy intervals is reported. From the Table it results that the response distorsion is considerable at low and high energy, while at intermediate energy it is not effective, since the absorption percentages in each channel are nearly constant.

TABLE III - Range telescope response for three different energy intervals: R is the ratio between incoming and detected protons in each channel; ΔR is the error on R, due to statistical fluctuations; proton losses due to nuclear absorption are reported in the third column.

Energy interval of each channel (MeV)	R	ΔR	Absorption percentage
93.4595 - 95.4169	0.9468	0.0457	0.0934
95.4169 - 97.3461	0.9238	0.0471	0.1111
97.3461 - 99.2460	0.9218	0.0480	0.1023
99.2460 - 101.1232	0.8720	0.0451	0.1555
101.1232 - 102.9736	0.8496	0.0442	0.1715
102.9736 - 104.7988	0.8648	0.0458	0.1450
104.7988 - 106.6004	0.8524	0.0448	0.1559
122.0350 - 123.6413	0.8368	0.0421	0.1950
123.6413 - 125.2352	0.8450	0.0420	0.1782
125.2352 - 126.8204	0.8244	0.0417	0.1964
126.8204 - 128.3903	0.8289	0.0413	0.1896
128.3903 - 129.9461	0.8131	0.0416	0.2040
129.9461 - 131.4996	0.8008	0.0407	0.2078
131.4996 - 133.0361	0.8190	0.0418	0.1880
204.0446 - 205.1849	0.8740	0.0425	0.1718
205.1849 - 206.3208	0.8387	0.0419	0.1835
206.3208 - 207.4520	0.8400	0.0404	0.1844
207.4520 - 208.5790	0.8405	0.0406	0.1835
208.5790 - 209.7019	0.7709	0.0396	0.2464
209.7019 - 210.8192	0.6734	0.0355	0.3412
210.8192 - 211.9378	0.6900	0.0357	0.3260

In Fig. 5 proton spectrum measured by the range telescope for photon energy E_γ = 200 MeV and for only one angular channel is reported.

The curve is the result of a calculation which takes into account:

1) photon incoming spectrum;
2) kinematics effects;
3) proton energy loss in liquid deuterium;
4) range telescope response function.

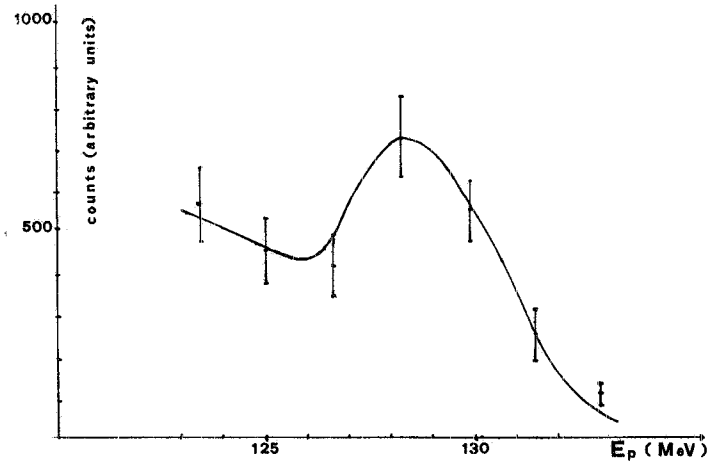

FIG. 5 - Proton spectrum measured by the range telescope for proton energy E_γ = 200 MeV and for one angular channel (θ_p = 30.83°) (solide angle 3.83 msterad). The solid curve is the result of a calculation which takes into account the photon incoming spectrum, kinematics effects, proton energy loss in liquid deuterium and the range telescope response function.

REFERENCES.

(1) - G. P. Capitani, E. De Sanctis, P. Di Giacomo, C. Guaraldo, R. Scrimaglio, P. Corvisiero, G. Ricco, M. Sanzone and A. Zucchiatti, Few body systems and electromagnetic interactions, ed. by C. Ciofi degli Atti and E. De Sanctis, Lecture Notes in Physics 86 (Springer, 1978), p. 128.
(2) - H. Arenhövel and W. Fabian, Few body systems and electromagnetic interactions, ed. by C. Ciofi degli Atti and E. De Sanctis, Lecture Notes in Physics 86 (Springer, 1978), p. 85; H. J. Weber and H. Arenhövel, Phys. Rep. 36C, 277 (1978); A. M. Green, Rep. on Progr. in Phys. 39, 1109 (1976).
(3) - M. Danos, Interaction studies in nuclei, ed. by N. Jochim and B. Ziegler, Mainz, 1975 (North Holland, 1975), p. 885.
(4) - G. P. Capitani, E. De Sanctis, P. Di Giacomo, C. Guaraldo, G. Ricco, M. Sanzone, R. Scrimaglio and A. Zucchiatti, Frascati Report LNF-77/35 (1977).
(5) - A. Zucchiatti, M. Sanzone and E. Durante, Nuclear Instr. and Meth. 129, 467 (1975).
(6) - R. Giordano, Nuclear Instr. and Meth. 95, 371 (1971).
(7) - D. F. Measday and C. Richard-Serre, CERN Report 69-17 (1969).
(8) - J. B. Marion and B. A. Zimmerman, Nuclear reactions analysis. Graphs and tables (North Holland, 1968).